# Numerical and Parametric Analysis of Horizontal Displacement and Distortions in Unreinforced Embankments on Soft Soils

Laura Zappellini Sassi
Civil engineering undergraduate student, UFSC, Florianópolis, Brazil, lazasassi@gmail.com

Naloan Coutinho Sampa
Professor, UFSC, Florianópolis, Brazil, naloan.sampa@ufsc.br

Tamara Bittencourt Corrêa
Civil engineering undergraduate student, UFSC, Florianópolis, Brazil, tamara.bitten@gmail.com

ABSTRACT: This paper, the second in a series of three, examines the horizontal displacement and distortion in four unreinforced embankments on soft soils using numerical and parametric analyses. The performance of granular embankments, each measuring 3.5 meters in height and 17 meters in width, on a soft soil layer extending 30 meters horizontally and with a thickness ranging from 5 to 20 meters was evaluated using Abaqus software. The soft clay and granular embankment material were modeled as elastoplastic, adhering to the Modified Cam Clay plasticity criterion and Mohr-Coulomb criterion, respectively. Forty numerical simulations were performed, encompassing various geometries and soil properties. The results present and discuss the impact of soil thickness, over-consolidation ratio (OCR), recompression index (k), and critical state slope (M) on horizontal displacement, distortion, and horizontal volume over 1-month and 48-month intervals. Furthermore, the paper analyzes the volume ratio, the displacement ratio, the pattern of horizontal displacement over time and along the depth, and the variations in normalized horizontal displacement and distortions along the depth for different vertical lines to identify patterns associated with slope instability.

KEYWORDS: Abaqus, Horizontal Displacement, Numerical Analysis, Parametric Analysis, Soft Soil, Unreinforced Embankments.

## 1 INTRODUCTION

Several researchers, including Hutchinson and Johnston (1973), Marche and Chapuis (1974), Matsuo and Kawamura (1977), and Bourges and Mieussiens (1979), have investigated the safety of instrumented embankments by assessing volumetric, horizontal, and total displacements. Their analyses facilitate the monitoring of embankment performance, prediction of potential failures, and formulation of interventions to ensure project success.

Hutchinson and Johnston (1973) observed that a ratio of vertical to horizontal volumes of soil ($V_v/V_h$) greater than 3.5 is indicative of stability. Marche and Chapuis (1974) proposed the dimensionless parameter $R$, estimated based on horizontal displacements, to evaluate stability. $R$ values lower than 0.16 are associated with low horizontal displacements, indicating safety factors greater than 1.4. Matsuo and Kawamura (1977) conducted numerical studies and proposed an evaluation method based on different percentages of failure, using vertical displacement ($\rho$) at the center of the embankment and superficial horizontal displacements ($\delta_h$) at the toe of the embankment.

Tavenas et al. (1979) investigated the correlation between $\delta_{h,máx}$ and $\rho_{máx}$ and found that values of $\delta_{h,máx}/\rho_{máx}$ ranging from 0.09 to 0.27 indicate approximately elastic behavior of the soil (pre-consolidated), while values between 0.71 and 1.31 indicate elasto-plastic behavior (normal consolidated). Furthermore, values in the constant range of 0.14 to 0.18 correspond to the consolidation phase.

Loganathan et al. (1993) introduced the FDA (Field Deformation Analysis) method, which involves determining parameters $\alpha$ and $\beta$ to characterize the ratios between vertical and horizontal displacements during the consolidation and creep stages, respectively. Additionally, Ladd (1991) outlined methodologies for analyzing the behavior and monitoring of embankments on soft soils. These methods encompass predicting shear trend zones, identifying failure zones, verifying drained or undrained responses, and assessing potential failures attributed to undrained shear.

Sandroni et al. (2004) proposed an empirical method based on $V_v/V_h$ over time ($t$) and embankment height ($H$). Analyzing this relationship along with the rate of change ($dV_v/dV_h$) over time can provide insight into failure trends. For example, during the loading phase, stability is indicated by ($V_v/V_h$) e de ($dV_v/dV_h$) values greater than 3, while values tending toward 1 indicate a state of failure or progressive failure. In the consolidation phase, characterized by constant loading and predominantly undrained behavior, stability is indicated by ($V_v/V_h$) e de ($dV_v/dV_h$) values greater than 5, while lower values warrant greater caution.

Distortion and distortion rate analysis, as described by Brugger (1996) and Almeida and Marques (2014), are additional methods for analyzing and monitoring the behavior of embankment on soft soils. Brugger (1996) addressed various aspects, including zones within the soil characterized by consolidation and creep, the influence of stiffness, consolidation, and creep on deformation. Additionally, they challenged the claim of Loganathan et al. (1993) regarding the reduction of horizontal displacement during consolidation due to excess pore pressure dissipation, and provided ranges of distortion and the ratio $\delta_{h,máx}/\rho_{máx}$ to evaluate embankment safety. On the other hand, Almeida and Marques (2014) introduced distortion rate values for the purpose of embankment monitoring and stability analysis.

This study aims to address existing gaps in the numerical modeling of embankments on soft soils by analyzing the displacement, volume, and distortion patterns of unreinforced embankments through numerical modeling and parametric analysis. The results obtained and discussed are of considerable importance for future investigations of the performance of embankments on homogeneous soft soils.

## 2 METHOD

### 2.1 Models Description

The numerical analysis of four unreinforced embankments on soft soils was performed using Abaqus software and assuming the plane strain condition. The 2D models consisted of a 3.5 m deep and 17 m long embankment of granular material with a slope of 1:2 (vertical to horizontal) over a soft clay layer 30 m long and 5 to 20 m thick. Due to the symmetry of the model, only half of the domain was simulated, as shown in Figure 1, where $H_s$ represents the thickness of the soft soil layer.

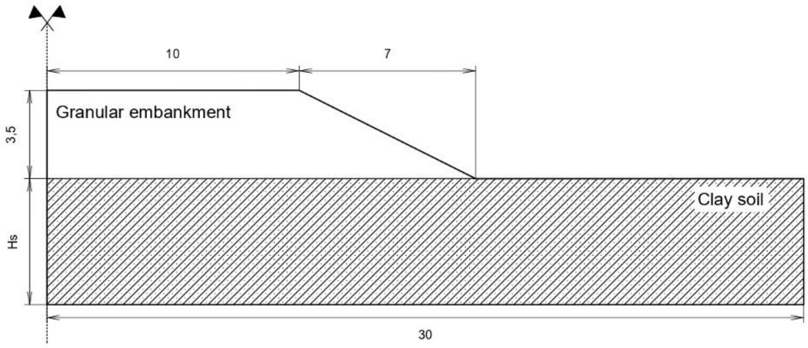


Figure 1. Half-domain of the numerical model of the embankment on the soft soil, in m.

### 2.2 Geotechnical Parameters

The soft clay was modeled as a homogeneous solid with elastoplastic behavior using the Modified Cam Clay plasticity criterion. Conversely, the granular embankment material was simulated in a dry state as a homogeneous solid body using the Mohr-Coulomb criterion. The geotechnical parameters for both the granular material and the clay soil are given in Table 1, where the clay parameters are typical of certain regions in Florianópolis, Brazil, as presented by Oliveira, 2006 and Baran, 2014.

Table 1. Geotechnical parameters of the soft soil and granular material.

| Granular material of the embankment | | Clay soil | |
|---|---|---|---|
| Parameter | Value | Parameter | Value |
| Initial void ratio - $e_0$ | 0.65 | Initial void ratio - $e_0$ | 2.5 |
| Bulk unit weight - $\gamma$ (kN/m³) | 20 | Bulk unit weight - $\gamma$ (kN/m³) | 15 |
| Cohesion - $c$ (kN/m²) | 2 | Recompression index - $\kappa$ | 0.065 |
| Internal friccional angle - $\phi$ (º) | 30 | Poisson's ratio - $\nu$ | 0.33 |
| Dilatancy angle - $\psi$ (º) | 0 | Compression index - $\lambda$ | 0.65 |
| Elastic Module - $E$ (kN/m²) | 1000 | Slope of the critical state line - $M$ | 1 |
| Poisson's ratio - $\nu$ | 0.3 | Overconsolidation ratio - OCR | 0.75, 1.0, 1.5, 3.0 |
| Permeability coefficient - $k$ (m/s) | 0.01 | Size of the yield surface in the wet side - $\beta$ | 1 |
| | | Ratio of the flow stress - $K$ | 1 |
| | | Permeability coefficient - $k$ (m/s) | 2.50E-08 |
| | | Lateral earth pressure at rest – $K_0 = 1 - \text{sen}\,\phi$ | 0.57 |

### 2.3 Simulation Sequences

The numerical simulations consisted of three stages, reflecting the sequential construction process of the single-phase embankments. The first stage involved the application of the Body Force option to stablish the initial geostatic stresses within the soft soil. The second stage then involved the gradual construction of the embankment to a height of 3.5 meters over a period of one month. Finally, the third phase involved monitoring the embankment's performance, including measuring vertical and horizontal displacements and excess pore water pressure, over a period of 48 months (4 years).

### 2.4 Boundary Conditions and Mesh Discretization

Physical and drainage boundary conditions were set to accurately simulate real embankment conditions under plane strain. For the physical boundary conditions, horizontal (U1=0) and vertical (U2=0) displacements were fixed at the bottom, while horizontal displacement (U1=0) was constrained at the right and left sides. Throughout the simulation, the soft soil surface maintained a zero pore pressure (U8=0) as part of the drainage boundary conditions.

Figure 2 illustrates the physical boundary conditions and mesh configuration of the numerical model with a 5 m thick layer of soft soil. The mesh has been refined particularly in areas where significant stresses and strains are expected.

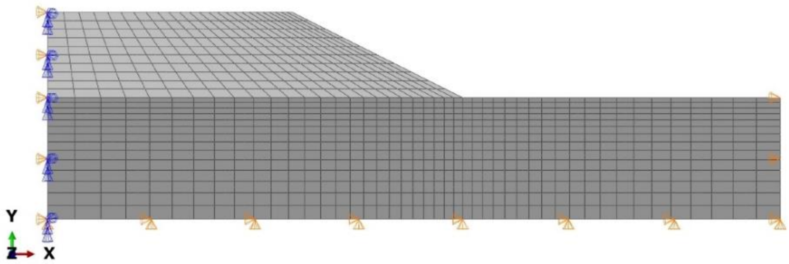


Figure 2. Boundary conditions and mesh discretization.

The numerical model used finite elements of type CPE8R (a quadrilateral flat deformation element with 8 nodes, bi-quadratic displacement, and reduced integration) for the embankment domain, and CPE8RP (a quadrilateral flat deformation element with 8 nodes, bi-quadratic displacement, bilinear pore pressure, and reduced integration) for the foundation domain.

### 2.6 Parametric Analysis

To investigate the effect of soil parameter variation on embankment performance, 10 parametric analyses were performed for each soil thickness ($H_s$=5, 10, 15 and 20 m), resulting 40 analyses. The parameters varied included the slope of the critical state line ($M$), the recompression index ($\kappa$), the overconsolidation ratio ($OCR$), and the soft soil thickness ($H_s$). Table 2 shows the parameters varied for each analysis and their respective values. Analysis 1 used parameters set to reference values, while subsequent analysis varied individual parameter values while holding others constant (for example: analysis 2 considers M=1.1, κ=0.065 and OCR=1.00).

Table 2. Parametric analysis.

| Analysis | M | Analysis | κ | Analysis | OCR |
|---|---|---|---|---|---|
| **Analysis 1 (reference)** | **1.0** | **Analysis 1** | **0.065** | **Analysis 1** | **1.00** |
| Analysis 2 | 1.1 | Analysis 5 | 0.050 | Analysis 8 | 0.75 |
| Analysis 3 | 1.2 | Analysis 6 | 0.080 | Analysis 9 | 1.50 |
| Analysis 4 | 1.3 | Analysis 7 | 0.095 | Analysis 10 | 3.00 |

The displacements and pore pressure results were evaluated over time, depth, and width. Figure 3 shows 11 designated points (A, B, C, D, E, F, G, H, I, J, and K) along with three horizontal lines (LH1, LH2, and LH3) and six vertical lines (LV1, LV2, LV3, LV4, LV5, and LV6) where data extraction from Abaqus to Excel was performed. Point data analysis was performed over time, horizontal line data analysis was performed over width, and vertical line data analysis was performed over depth.

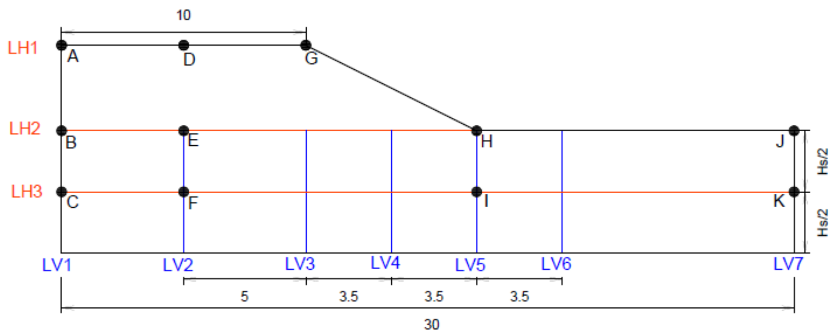


Figure 3. Points and lines of interest for data extraction, in m.

## 3 RESULTS AND DISCUSSION

The ratio of horizontal to vertical displacement ($\delta_h/\rho$) is critical in evaluating slope performance. Figure 4 shows the spatial distribution of horizontal displacement for analysis 1 with a slope height ($H_s$) of 5 m at 1 month and 48 months. Excessive horizontal displacement ($\delta_h$), especially relative to vertical displacement ($\rho$), can lead to the development of shear stress zones and embankment failure, as highlighted by the red area in Figure 4, which indicates higher horizontal displacement values within the soft soil beneath the slope.

Due to space limitations, only selected typical figures are presented. However, the discussions cover the behavior observed in all 40 analyses performed.

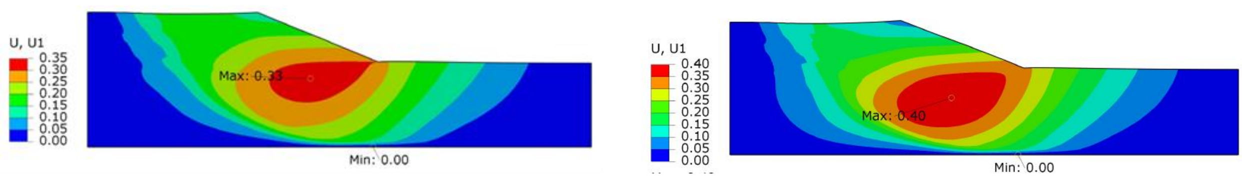


(a) Horizontal displacement at 1 month. (b) Horizontal displacement at 48 months.

Figure 4. Spatial distribution of the horizontal displacement.

The variation of horizontal displacement ($\delta_\mathrm{h}$) and normalized horizontal displacement ($\delta_\mathrm{h}/H_\mathrm{e}$) was examined along the depth of three vertical lines - LV3, LV5 and LV6 - at time intervals of 1 month and 48 months. Figure 5 shows the typical variation of $\delta_\mathrm{h}/H_\mathrm{e}$ along the normalized depth ($z/H_\mathrm{s}$) of LV5 for some analyses with $H_\mathrm{s}$ of 5 m and 10 m, varying $OCR$ values. In models with a soil thickness ($H_\mathrm{s}$) of 5 m, the horizontal displacement increases after the completion of the embankment construction, as stated by Brugger (1996). Conversely, models with soil thicknesses of 10, 15, and 20 m show an opposite trend, consistent with the observation of Loganathan et al. (1993), where horizontal displacement decreases during consolidation. Further detailed analyses are required to understand the primary reasons for the reversal of horizontal displacement, despite Brugger (1996) associating this phenomenon with limitations in some numerical modeling.

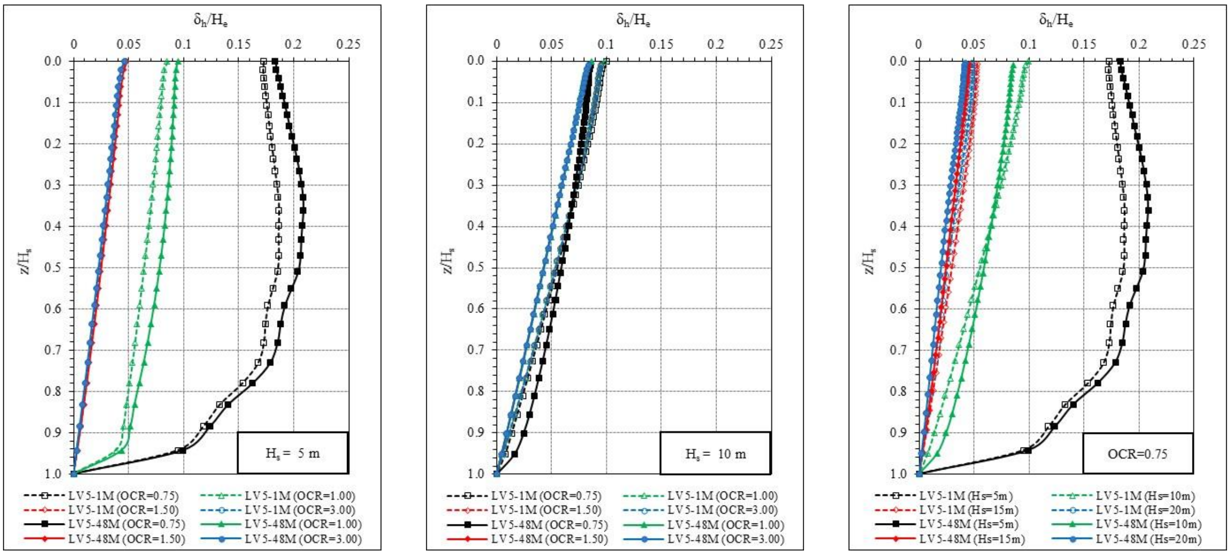

(a) (b) (c)

Figure 5. Variação de $\delta_\mathrm{h}/H_\mathrm{e}$ versus $z/H_\mathrm{s}$.

The maximum horizontal displacement [$(\delta_\mathrm{h}/H_\mathrm{e})_\mathrm{max}$] typically occurs at the surface of the soft soil ($z/H_\mathrm{s} = 0$), except for line LV3 in some analyses with $H_\mathrm{s} = 5$ m. In these cases, $\delta_\mathrm{h}/H_\mathrm{e}$ tends to remain constant between $z/H_\mathrm{s}$ of 0.1 to 0.7, decreasing thereafter to zero at $z/H_\mathrm{s} = 1$. In most cases, they tend to exhibit a curvilinear pattern. Conversely, $\delta_\mathrm{h}/H_\mathrm{e}$ tends to decrease linearly from its maximum value at the surface ($z/H_\mathrm{s}$ = 0) to zero at $z/H_\mathrm{s}$ = 1. It is pertinent to note that the boundary condition constrained the horizontal displacement at the bottom of the model ($z/H_\mathrm{s} = 1$). Considering that analyses with $H_\mathrm{s} = 20$ m demonstrate $\delta_\mathrm{h}/H_\mathrm{e}$ at greater depths, it is reasonable to infer that $\delta_\mathrm{h}/H_\mathrm{e}$ at the base of models with $H_\mathrm{s}$ of 5 m, 10 m and 20 m tend to exceed zero. In other words, the results underscore the inadequacy of all soft soil thicknesses in constraining horizontal displacement at the bottom of the models. Therefore, conducting additional analyses without constraints on horizontal displacement at the bottom would be appropriate to elucidate this behavior.

Regardind the parametric analyses, it was observed that the variations in $M$ and $OCR$ only affect $\delta_\mathrm{h}/H_\mathrm{e}$ for $H_\mathrm{s} = 5$ m. When varying parameter $M$ along LV5, $(\delta_\mathrm{h}/H_\mathrm{e})_\mathrm{max}$ ranges from 5.5% to 9.5% for $H_\mathrm{s} = 5$ m, and from 8.7% to 4.4% for $H_\mathrm{s} = 10$ m, 15 m, and 20 m. Similarly, when varying the $OCR$ parameter along LV5, $(\delta_\mathrm{h}/H_\mathrm{e})_\mathrm{max}$ ranges from 4.6% to 21.0% for $H_\mathrm{s} = 5$ m, and from 8.4% to 4.2% for $H_\mathrm{s} = 10$ m, 15 m, and 20 m. The variation of parameter $\kappa$ influences $\delta_\mathrm{h}/H_\mathrm{e}$ for all $H_\mathrm{s}$ values, with increasing $\kappa$ leading to increased horizontal displacement. Along LV5 line, $(\delta_\mathrm{h}/H_\mathrm{e})_\mathrm{max}$ varies from 7.7% to 12.5%, 6.5% to 12.7%, 3.7% to 7.3%, and 3.1% to 6.3% for $H_s = 5$ m, 10 m, 15 m, and 20 m, respectively.

In most cases, $(\delta_\mathrm{h}/H_\mathrm{e})_\mathrm{max}$ is below 10%. However, there was a critical situation in the analyses with $OCR = 0.75$ and $H_\mathrm{s} = 5$ m where $(\delta_\mathrm{h}/H_\mathrm{e})_\mathrm{max}$ reached 21%.

Variations in $M$ and $\kappa$ minimally impact the magnitude of the decrease in horizontal displacement during consolidation for models with $H_s \geq 10$ m. Variation in $OCR$ has a greater impact on the reversal of the horizontal displacement than $M$, which in turn exceeds the influence of variation in $\kappa$.

Regarding the ratio $\delta_{\text{h,máx}}/\rho_{\text{máx}}$, it is noted that at the end of embankment construction (1 month), it varies between 0.318 and 0.652 in analyses with $H_s = 5$ m, between 0.459 and 0.561 in analyses with $H_s = 10$ m, between 0.328 and 0.409 in analyses with $H_s = 15$m, and between 0.275 and 0.341 in analyses with $H_s = 20$ m. At the end of consolidation, the ratio $\delta_{\text{h,máx}}/\rho_{\text{máx}}$varies between 0.184 and 0.474 in analyses with $H_s = 5$ m, between 0.234 and 0.274 in analyses with $H_s = 10$ m, between 0.197 and 0.212 in analyses with $H_s = 15$ m, and between 0.164 and 0.169 in analyses with $H_s = 20$ m. The ratio $\delta_{\text{h,máx}}/\rho_{\text{máx}}$ decreases with increasing $H_s$, and only the results of analyses with $H_s$ of 5 m are significantly affected by variations in parameters $M, \kappa,$ and $OCR$. It is important to note that analyses with $\delta_{\text{h,máx}}/\rho_{\text{máx}}$ between 0.09 and 0.27 indicate approximately elastic behavior of the soil, while those with $\delta_{\text{h,máx}}/\rho_{\text{máx}}$ between 0.71 and 1.31 correspond to elasto-plastic behavior, as stated by Tavenas et al. (1979).

Figure 6 shows the variation of the total distortion, calculated as $\text{atan}\{(\delta_{\text{h}2} - \delta_{\text{h}1})/(z_2 - z_1)\}$, along the normalized depth. The variation in parameters $M$ and $OCR$ affect the percentage of total distortion in analyses with $H_s = 5$ m. Regardless of the $H_s$ value, an increase in $\kappa$ results in increased total distortion in lines LV3, LV5, and LV6, with the total distortion varying along depth depending on line position.

In analyses with $H_s = 5$ m, total distortion tends to increase slightly with normalized depth. With the exception of analyses where $OCR = 0.75$, most analyses with $H_s = 5$ m have a maximum total distortion of less than 10% at $z/H_s$ below 0.85. Conversely, for analyses with $H_s \geq 10$ m, the total distortion stabilizes at greater depths and typically remains below 2%, especially for analyses with $H_s$ of 15 m and 20 m.

The total distortion decreases as the soft soil thickness increases, particularly when $H_s \geq 10$ m. For normalized depths less than 0.45, the deformations in analyses with $H_s = 5$ m are less than those in analyses with $H_s = 10$ m. In all analyses, the deformation rate remains well below 0.5% per day, indicating slope stability as reported by Almeida and Marques (2014).

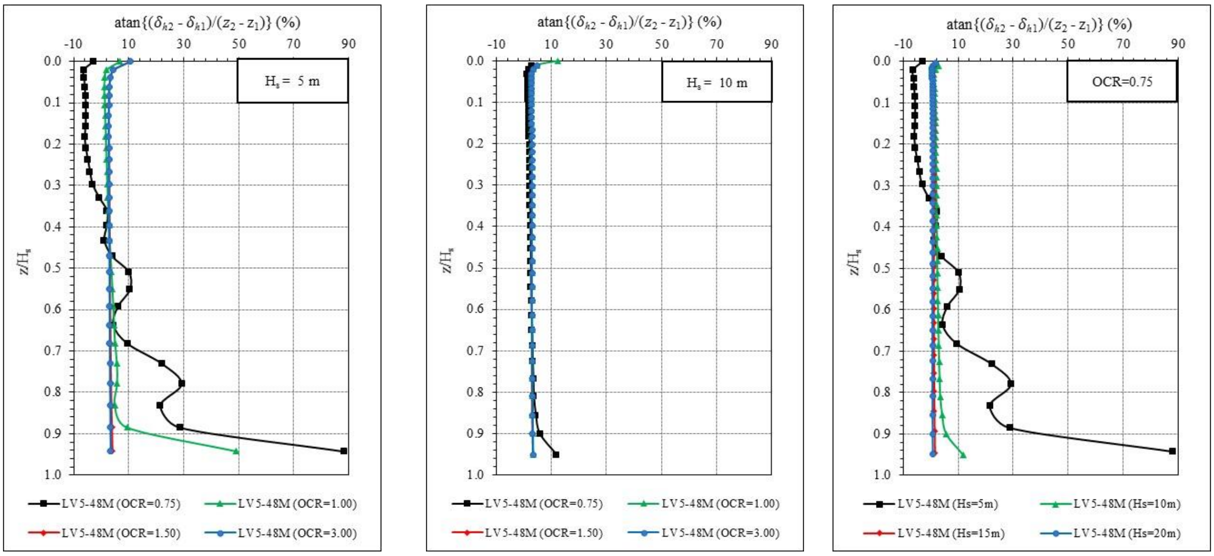


(a) (b) (c)

Figure 6. Distortion versus $z/H_s$.

Figures 8a - 8f show the effect of parameter variations on the ratio between volumes. The analyses included the vertical volume of soil mobilized below the embankment ($V_{\text{v}1}$), the vertical volume of soil mobilized above the embankment toe ($V_{\text{v}2}$), and the horizontal volume of soil mobilized along line LV5 ($V_{\text{h}}$). The trend observed in $V_{\text{h}}$ mirrors that of horizontal displacement. Specifically, in models with $H_s = 5$m, $V_{\text{h}}$ continues to increase after embankment construction, whereas in analyses with $H_s = 10$ m, 15 m, and 20 m, $V_{\text{h}}$ shows a decrease after completion of embankment activities.

As expected, both the horizontal displacement ($\delta_{\text{h}}$) and the horizontal volume ($V_{\text{h}}$) decrease with the distance from the creast of the slope. Specifically, the $V_{\text{h}}$ values of line LV3 are higher than those of line LV5, which are higher than those of line LV6.

For $H_s \geq 10$ m, both $V_{\text{h}}$ and $V_{\text{v}1}$ decrease slightly with increasing $H_s$ and remain relatively stable with variations in $M$, $\kappa$, and $OCR$. Conversely, for analyses with $H_s = 5$ m, $V_{\text{h}}$ and $V_{\text{v}1}$ tend to decrease with increasing $M$ and $OCR$, while increasing with increasing $\kappa$.

At 48 months (and 1 month), $V_\mathrm{h}$ ranges between 0.18 m³ and 1.68 m³ (0.21 m³ and 1.61 m³) for $H_\mathrm{s} = 5$ m, 0.56 m³ and 1.05 m³ (0.64 m³ and 1.50 m³) for $H_\mathrm{s} = 10$ m, 0.41 m³ and 0.79 m³ (0.52 m³ and 1.09 m³) for $H_\mathrm{s} = 15$ m, and 0.37 m³ and 0.70 m³ (0.48 m³ and 1.01 m³) for $H_\mathrm{s} = 20$ m.

Similarly, the vertical volume $V_{\mathrm{v}1}$ at 48 months (and 1 month) ranges between 3.39 m³ and 12.94 m³ (3.28 m³ and 8.69 m³) for $H_\mathrm{s} = 5$ m, 6.93 m³ and 12.35 m³ (6.92 m³ and 12.53 m³) for $H_\mathrm{s} = 10$ m, 6.10 m³ and 11.39 m³ (6.02 m³ and 11.15 m³) for $H_\mathrm{s} = 15$ m, and 5.47 m³ and 10.56 m³ (7.00 m³ and 12.90 m³) for $H_\mathrm{s} = 20$ m.

Furthermore, the ratio $V_{\mathrm{v}1}/V_\mathrm{h}$ at 48 months (and 1 month) varies between 7.69 and 22.97 (5.41 and 15.84) for $H_\mathrm{s} = 5$ m, 11.98 and 12.33 (8.33 and 9.40) for $H_\mathrm{s} = 10$ m, 13.05 and 13.79 (10.24 and 11.64) for $H_\mathrm{s} = 15$ m, and 16.27 and 16.71 (12.76 and 14.73) for $H_\mathrm{s} = 20$ m. The results are indicating the stability condition, since the $V_{\mathrm{v}1}/V_\mathrm{h}$ is greater than 3 at the end of the embankment construction and greater than 5 at the end of the consolidation, as recomended by Sandroni et al. (2004).

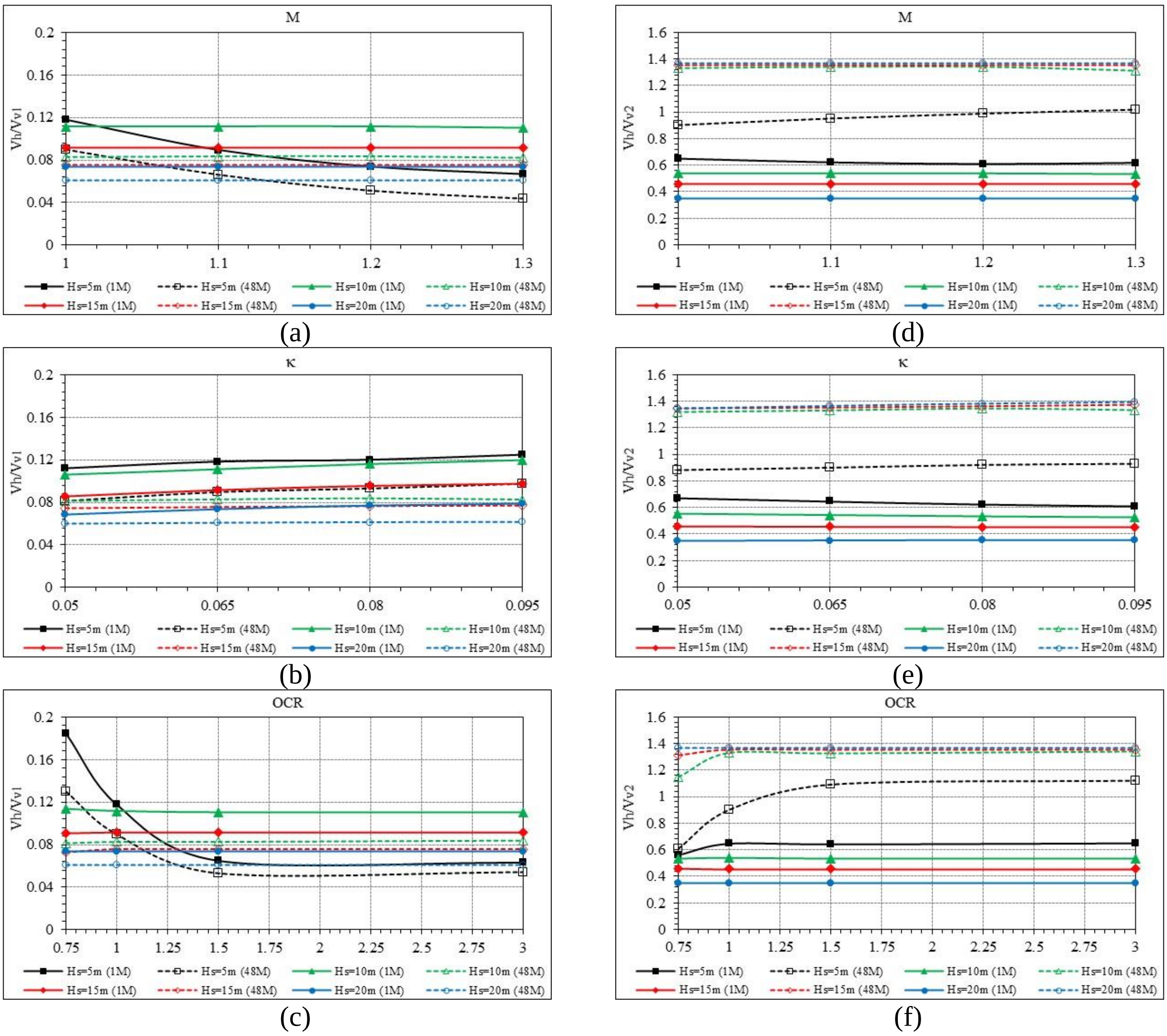


Figure 7. Análise paramétrica de volumes.

The behavior of the horizontal displacement reversal can be assessed by the ratio $V_{\mathrm{v}1}/V_{\mathrm{v}2}$. At 1 and 48 months, $V_{\mathrm{v}1}/V_{\mathrm{v}2}$ varies between 4.66 and 23.42 (3.02 and 10.28) for $H_\mathrm{s} = 5$ m, between 14.05 and 16.24 (4.36 and 5.17) for $H_\mathrm{s} = 10$ m, between 17.85 and 18.05 (4.59 and 5.35) for $H_\mathrm{s} = 15$ m, and between 22.47 and 22.61 (4.50 and 5.11) for $H_\mathrm{s} = 20$ m. Based on the results, it can be inferred that $V_{\mathrm{v}1}$ continues to increase after the completion of the embankment, whereas $V_{\mathrm{v}2}$ tends to decrease due to the reversal of horizontal displacement.

## 4 CONCLUSIONS

This paper presents the results of 40 numerical simulations that investigate the effects of the parameters $M$ – slope of the critical state line, $OCR$ – overconsolidation ratio, κ – recompression index, and $H_s$ - thickness of the soft soil layer, on the horizontal displacement, distortion, and volumes of the mobilized soft soil during analyses. The key conclusions are presented below:

- in models with $H_s$ of 5 m, $\delta_h$ increases after the completion of the embankment construction. Conversely, models with $H_s \geq 10$ m show an opposite trend;
- the variations in $M$ and $OCR$ only affect $\delta_h/H_e$ for $H_s = 5$ m. The variation in $\kappa$ influences $\delta_h/H_e$ for all $H_s$ values, with increasing $\kappa$ leading to increased $\delta_h/H_e$. Most analyses indicate that the results of models with $H_s = 5$ m do not follow the trend of those of models with $H_s \geq 10$ m;
- in most cases, $(\delta_h/H_e)_{max}$ is below 10%. However, there was a critical situation in the analyses with $OCR = 0.75$ and $H_s = 5$ m where $(\delta_h/H_e)_{max}$ reached 21%;
- Variations in $M$ and $\kappa$ minimally impact the magnitude on the reversal of the horizontal displacement during consolidation for models with $H_s \geq 10$ m;
- the ratio $\delta_{h,máx}/\rho_{máx}$ decreases with increasing $H_s$, and only the results of analyses with $H_s$ of 5 m are significantly affected by variations in parameters $M, \kappa,$ and $OCR$;
- regardless of the $H_s$ value, an increase in $\kappa$ results in increased total distortion;
- the total distortion decreases as $H_s$ increases, particularly when $H_s \geq 10$ m;
- for $H_s \geq 10$ m, both $V_h$ and $V_{v1}$ decrease slightly with increasing $H_s$ and remain relatively stable with variations in $M$, $\kappa$, and $OCR$. Conversely, for analyses with $H_s = 5$ m, $V_h$ and $V_{v1}$ tend to decrease with increasing $M$ and $OCR$, while increasing with increasing $\kappa$.

## REFERENCES

Almeida, M.S.S., Marques, M. E. S. (2014) *Aterros sobre solos moles: projeto e desempenho*. São Paulo: Oficina de Textos.

Baran, Karin. *Propriedades geotécnicas de compressibilidade de uma argila mole de Itajaí, SC*. 2014. 334 f. Dissertação (Mestrado) – Curso de Engenharia Civil, Universidade Federal de Santa Catarina, Florianópolis, 2014.

Bourges, F., Mieussens, C. (1979) *Influence des déplacements lateraux du sol de foundation sur le tassements d'un remblai*, Bulletin de Liaison, Laboratorire des Ponts et Chaussées.

Brugger, P.J. *Análise de deformações em aterros sobre solos moles*. Doctor of Philosophy, Department of Science of Civil Engineering, Federal University of Rio de Janeiro, 1996.

Hutchinson, J.N., Johnston, I.W. (1973) [Discussion]. *In: Symposium Fiel instrumentation in Geotechical Engineering*. London, Proceedings… London, ICE, p. 700-702.

Ladd, C.C. (1991) *Stability evaluation during staged construction*. Journal of Geotechnical Engineering, v. 117 (4), p. 537-615.

Loganathan, N., Balasubramaniam, A.S., Bergado, D.T. (1993) D*eformation analysis of embankments*. Journal of Geotechnical Engineering, v. 119 (8), p. 1185-1206.

Marche, R., Chapuis, R. (1974) *Contrôle de la stabilité desremblais par la mesure des displacements horizontaux*. Canadian Geotechnical Journal, v. 11, p. 182-201.

Matsuo, M., Kawamura, K. *Diagram for construction control of embankment on soft ground*, Soils and Foundations, v. 17 (3), p. 25-35.

Oliveira, Henrique de. *Comportamento de aterros reforçados sobre solos moles levados à ruptura*. 2006. 507 f. Tese (Doutorado) - Curso de Engenharia Civil, Universidade Federal do Rio de Janeiro, Rio de Janeiro, 2006.

Sandroni, S.S., Lacerda, W.A., Brandt, J.R.T. (2004) *Método dos volumes para controle de campo da estabilidade de aterros sobre argilas moles*. Soils and Rocks, São Paulo, v. 27 (1), p. 25-35. [in Portuguese]

Tavenas, F., Mieussens, C., Bourges, F. (1979) *Lateral displacements in clay foundations under embankments*. Canadian Geotechnical Journal, v. 16, p. 532-550.